

A Predictive Model Accounting for the Mechanical Behavior of Galvanized Alloy Layers on the Mild Steel

H. Sharifi *

Faculty of Engineering, Shahrekord University, Shahrekord, Iran

Abstract

Zinc coating is formed by the heterogeneous assembly of the Γ , Γ_1 , δ , ζ and η phases whose mechanical properties greatly differ from each other. Thermal strains resulting from large differences between thermal expansion coefficients are partially relaxed by the formation of a crack network. In order to model this phenomenon, initial hardness, thermal expansion coefficient α_i and toughness (K_{IC}) of the phases were determined. Hardness testing experiments performed on the galvanizes samples with and without annealing revealed that during the cooling down of the samples in the coating process, there was some residual stress in the coating due to the difference between the thermal expansion coefficients of the phases. In this regard, maximum hardness, 340 HV, was obtained for δ phase and its toughness was measured to be about $2\text{MPa}\sqrt{\text{m}}$, thereby revealing that δ phase was completely brittle compared to other phases. Modeling the behavior of the phases present in the coating demonstrated that during the cooling stage, at first, some micro-cracks were formed in δ phase and grew in two stages: I) perpendicular to the δ/α interface and II) parallel to the δ/α interface. The results revealed that when the thickness of δ phase was more than $5\mu\text{m}$, there was a good agreement between the experimental results and the proposed model. Also, due to the properties of the coating layers, the resulted stresses could not delaminate the coating.

Keywords: Modeling, Galvanizing, Intermetallic, Alloy layers, Toughness, Residual stress.

1. Introduction

Galvanizing is a process for rustproofing iron and steel by the application of a zinc coating. Three of the most widely-used processes for applying zinc to iron and steel are hot-dip galvanizing, electrogalvanizing and zinc spraying. Most products are coated using the hot-dip process. It involves immersing steel into a bath of molten zinc that is at a temperature close to 465°C (870°F) in order to form a metallurgically bonded zinc or zinc-iron alloy coating. This same hot-dip immersion process is also used to produce other coatings such as zinc-aluminum alloys ¹⁻⁴.

Hot-dip galvanizing is known as the most common technique for the protection of steel sheets and structural sections from atmospheric corrosion although it can affect the forming characteristics of steels ⁵.

The Zn-Fe binary system is shown in Fig. 1 ⁶. Enough evidence is, however, available to show that the coated layer in the hot dip galvanized iron is not a

single phase region; rather, it consists of several layers of various phases found in the Fe-Zn phase diagram, as shown schematically in Fig. 2. When subjected to shear force, this composite assembly of the phases is expected to behave in a substantially different way compared to the pure Fe-Zn system considered earlier. In fact, the shear resistances at the interfaces between any two pair of phases are expected to vary significantly as both their crystal structures and hardness values are known to be widely different ^{5,7}.

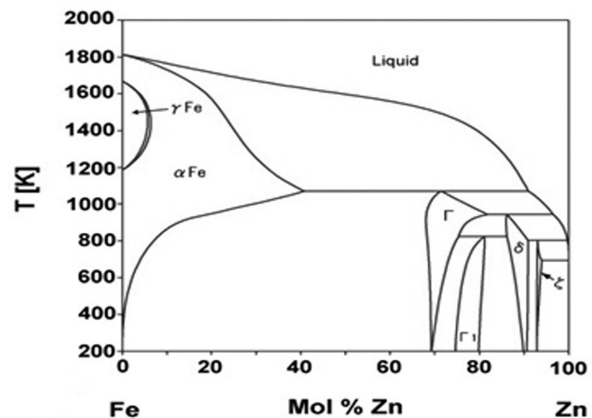


Fig. 1. The Zn-Fe phase diagram ⁶.

* Corresponding author

Tel: +98 913 109 4053

E-mail: Sharifi@eng.sku.ac.ir

Address: Faculty of Engineering, Shahrekord University, Shahrekord, Iran

Assistant Professor

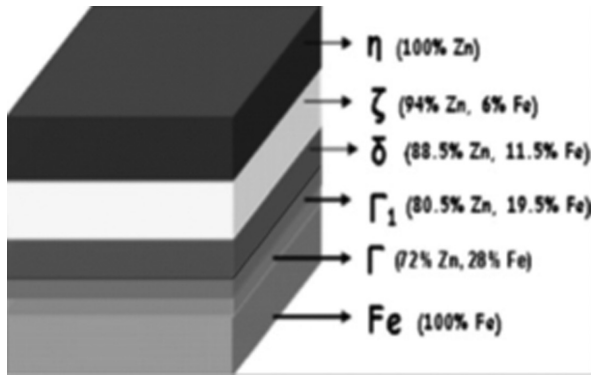


Fig. 2. Schematics of phases present in the zinc coated iron ^{5,7}.

However, zinc coating is a heterogeneous assembly of alloys and intermetallic compounds that have widely different mechanical properties. The characteristics of various phases in the coated layer are summarized in Table 1 ^{5,7}. Cracks formed during the cooling stage in the δ layer may or may not develop under service conditions ⁸. The aim of this paper was to show how crack formation and crack propagation could be modeled and under which condition, the crack network could not lead to any detrimental consequences.

Table 1. Characteristics of Fe–Zn intermetallic phases ^{5,7}.

Characteristics	η (Eta)	ζ (Zeta)	δ (Delta)	Γ_1 (Gamma)	Γ (Gamma)
Stoichiometry	Zn	FeZn ₁₃	FeZn ₁₀	Fe ₅ Zn ₂₁	Fe ₃ Zn ₁₀
Crystal Structure	HCP	Monoclinic	Hexagonal	FCC	BCC
Melting Point (°C)	419	530	665	550	782

2. Experimental Procedure

The chemical composition of low carbon steel substrates used in this investigation is listed in Table 2. At first, the samples with the dimensions of 30×10×5 mm³ were prepared and then the steels were polished and cleaned in alkaline solution for 15 minutes. This was followed by pickling in 50% HCl at 20°C for 15 minutes. Fluxing was accomplished by the immersion of the pickled steels in the ZnCl+NH₃Cl solution at 20 °C for 5 minutes. Before this operation, the fluxed steels were heated at 140 °C for 15 minutes. Hot dip galvanization was performed at 450 °C in pure zinc bath for up to one month. Three series of the samples were selected after galvanizing: T₁: without any heat treatment, T₂: heat treatment for 2 hours at 350 °C and T₃: heat treatment for 8 hours at 350 °C.

Table 2. Chemical composition of the low carbon steel(wt.%).

Substrate	C	Si	Mn	P	S	Al
Carbon steel	0.06	0.08	0.17	0.015	0.008	0.003

The hardness testing of the intermetallic phases of Fe -Zn was performed with a standard Vickers diamond pyramid indenter using loads from 5 to 2000 gf. In order to avoid surface compressive stresses, the specimens were carefully polished by mechanical grinding before the measurements of micro hardness. In order to minimize the dispersion, the hardness measurements were systematically repeated up to 10 times.

3. Results and Discussion

3.1. Microstructure of the coating

The coating consisted of a series of Fe-Zn intermetallic layers. First, very thin layers of Γ and Γ_1 in contact with the substrate were followed by a thicker compact δ phase and then superimposed by a ζ layer which was covered by the equiaxed zinc η -phase.

3.2. Mechanical properties

The hardness (HV) was found to be strongly dependent on the load (P) used. The dependence of hardness on the reciprocal length of the diagonal was linear (Fig. 3).

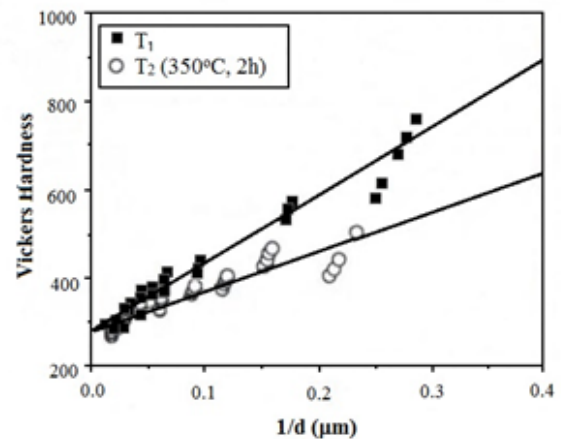


Fig. 3. Vickers hardness as a function of the reciprocal indentation diagonal for T₁ and T₂ samples. H₀ corresponds to the absolute hardness, and the slope, B, gives the dependence on the applied load.

Two parameters, H₀ and B, were necessary to describe the behavior of the material. H₀ corresponded to the hardness obtained at the very high load (macro-hardness domain) and B gave the dependence on the applied loads. The large value found for B in this case could be associated with the presence of residual stresses ^{9,10}. The decrease of B was observed when the sample was heat treated (T₂) in order to relax the internal stresses. Among the experimental conditions, only the duration of treatment was found to influence the hardness. This influence was not related to the intrinsic hardness (H₀~285 kgf/cm²), which remained constant, but it affected the value of B, thereby indicating the sensitivity to the applied load. This phenom

enon might be related to the increase in homogeneity resulting from longer treatments. In other phases, the apparent hardness (for a 5 gf applied load) was reduced compared with that in δ :

$$HV_{\delta} = 340, HV_{\zeta} = 112, HV_{Fe} = 150, HV_{zn} = 70 \quad (1)$$

It showed that δ phase was hard and very brittle. Microcracks were nucleated at the vicinity of the indent due to the sharp Vickers indenter, when the applied load was larger than a critical value, i.e., P_o .

Fig. 4 shows that surface radial cracks produced by indentation were significantly smaller in the annealed specimen than those in the as-cooled material. But the critical load necessary to initiate cracks was unchanged by the heat treatment.

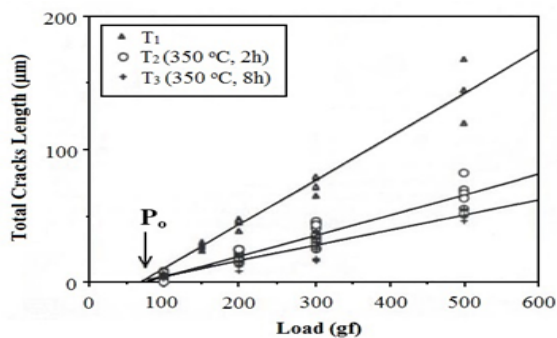


Fig. 4. Variations of crack length against the applied load for samples T_1 , T_2 and T_3 (the critical load, P_o , which was necessary to initiate cracks, was constant).

Surfaces cracks associated with Vickers indentation are now widely used to estimate the fracture toughness of brittle materials^{9,11-13}. For carefully annealed specimens (T_3), the values obtained varied from 1 to 2 MPa \sqrt{m} .

Fig. 5 shows the results obtained with the Evans and Charles formula¹⁴.

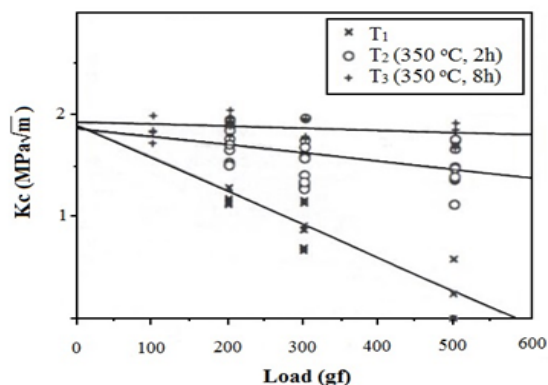


Fig. 5. Vickers indentation toughness versus the applied load.

The following value was chosen for the toughness: $K_{IC}^{\delta} = 2 \text{ MPa}\sqrt{m}$. In the experimental range, from 25 to 2000 gf for the applied load, the fracture toughness

was nearly constant. On the contrary, for treatment T_1 , it could be seen that the apparent toughness was decreased as the applied load (then the crack length, c) was increased. The existence of a strong negative dependence of K_c versus $1/\sqrt{c}$ over the load range and the independence of K_{IC} versus the applied load for the annealed specimen provided evidence for the tensile nature of residual stresses.

The determination of the residual stresses, σ_r , by means of indentation measurements has been proposed by Marshall and Lawn¹⁵. The apparent stress intensity factor, K_a , is considered to result from two contributions: $K_a = K_c + K_r$, where K_r is a function of σ_r :

$$K_a = K_c \pm 2\sigma_r \frac{\sqrt{c}}{\sqrt{\pi}} \quad (2)$$

By using a value of 2 MPa \sqrt{m} for K_c , a residual stress of 240 MPa can be obtained from the slope of K_a versus \sqrt{c} ¹⁵.

It is now well known that multilayers develop complex residual stresses during the cooling stage depending on the difference in the thermal expansion behavior and the elastic and plastic properties of the component. Thick intermetallic delta, zeta and eta-phases were obtained by galvanizing low carbon steels^{16,17} from 1 to 1.5 months. The thermal expansion coefficients α_i of the "i" intermetallic compounds were then determined by a linear differential transducer in the temperature range 20-60 °C. The heating rate was controlled to be less than 3-4 Kmin⁻¹. The values obtained were:

$$\alpha_i^{\delta} = 21.8 \times 10^{-6} \text{ K}^{-1}, \alpha_i^{\zeta} = 23.10 \times 10^{-6} \text{ K}^{-1}, \alpha_i^{\eta} = 25.60 \times 10^{-6} \text{ K}^{-1} \quad (3)$$

Approximately, a value twice larger was found for steel ($11.3 \times 10^{-6} \text{ K}^{-1}$) and the great difference observed suggested that hop-dip galvanized coatings developed substantial tensile thermal stresses during cooling. Such stresses could be easily visualized by the test described in Fig. 6. It can be seen that specimens galvanized on one side were bowed towards the coated side during cooling. It followed that residual stresses were generated during cooling and not during the galvanizing process, and corresponded to a tensile stress field in the intermetallic compounds. This was also proved by acoustic emission. In other galvanizing conditions, the stress resulting from unbalanced mass diffusion and the cracking may occur during the galvanizing reaction.

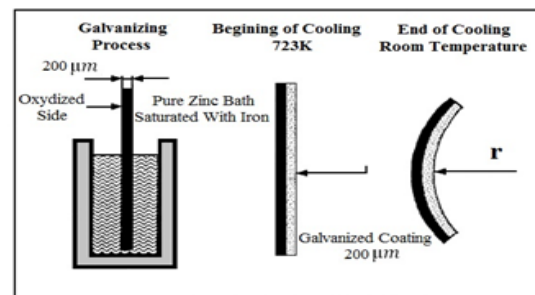


Fig. 6. A simple way to characterize the residual stresses.

A rough idea of the maximum tensile stress may be obtained by considering a beam of a bimetallic strip built up of delta-phase and iron. By assuming that there is no sliding between the two materials during bending, the maximum tensile stress in delta-phase can be calculated by means of the Timoshenko elastic relation¹⁸⁾. In this way, we can obtain a maximum surface stress of 490 MPa.

3.2. Modeling

Two clear observations were made: during cooling from reaction temperature to 20 °C, an initial crack network, I, was developed in δ and the propagation direction was perpendicular to the α/δ interface (Fig. 7b); under external tensile stress parallel to the α/δ interface, a second crack network, II, was developed from I, but it was inside δ and parallel to the α/δ interface.

3.3.1. Formation of crack network I

The crack network I resulted from the relaxation of the tensile thermal stresses in the coating during cooling. Two clear observations were made: during cooling from reaction temperature to 20 °C, an initial crack network, I, was developed in δ and the propagation direction was perpendicular to the α/δ interface (Fig. 7b); under external tensile stress parallel to the α/δ interface, a second crack network, II, was developed from I, but it was inside δ and parallel to the α/δ interface. The crack network I resulted from the relaxation of tensile thermal stresses in the coating during cooling.

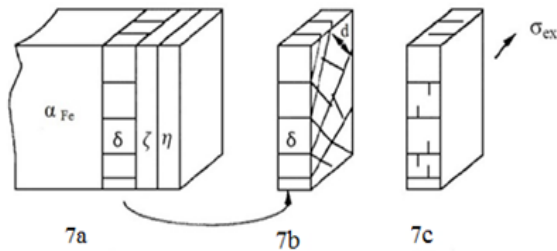


Fig. 7. During cooling, a crack network in the galvanizing coating was developed in the δ layer according to mode I propagation (7a and 7b). Under external stress, the propagation mode in δ became II (7c).

The large difference between thermal expansion coefficients was the cause of these large thermal stresses. If the system had not undergone any stress at the galvanizing temperature, the large contraction of the compounds would have had higher α than Fe, thereby creating important tensile thermal stresses. If these thermal strains σ_i^{th} could be accommodated elastically by different "i" layers separated interfaces, the stresses would be determined by the following equations:

$$\alpha_i \Delta T + \frac{\sigma_i^{th}}{E_i} = C_{st} \quad \sum \sigma_i t_i = 0 \quad (4)$$

The experimental observations showed that except in δ , the thermal strains were accommodated plastically; therefore, Eq. (4) is reduced to:

$$\alpha_\delta \Delta T + \frac{\sigma_\delta^{th}}{E_\delta} = \alpha_\alpha \Delta T \quad (5)$$

where σ_δ^{th} could be neglected because of the large thickness of iron compared with that of the δ layer. In order to emphasize the two sources of thermal stress in δ , i.e., ΔT and $\Delta\alpha = \alpha_\alpha - \alpha_\delta$, Eq. (5) is also written as follows:

$$\sigma_\delta^{th} = E_\delta \Delta T \Delta\alpha \quad (6)$$

Because the dimensions of the surface to be galvanized were much larger than t_δ , σ_δ^{th} corresponded to circular plane stresses. The thermal strain in δ , about 5×10^{-3} , could not be relaxed plastically by this phase, which was very brittle as proved above. The crack network I corresponded to cracks essentially propagating in mode I. Rather than a honeycomb shape, the crack network presented many right angles roughly corresponding to square cells with the length d . This orthogonal crack propagation was also consistent with plane stress: once a single crack was propagated along one direction, it became the principal axis of the stress field which then needed orthogonal cracks to be relaxed. Experimentally, the crack network I appeared to be square prismatic surface of the mean cell size d and the height t_δ . The total crack length observed per surface unit S_0 on a cross section of δ parallel to the α/δ interface could be represented by:

$$L \approx \frac{2S_0}{d} \quad (7)$$

The maximum thermal stress energy which is likely to be stored in δ is:

$$W_{max}^{th} = E_\delta (\Delta\alpha)^2 (\Delta T)^2 t_\delta S_0 \quad (8)$$

where E_δ is the Young modulus of δ , and the factor 1/2 disappears in accordance with the biaxial state of the stress field.

According to the previous determination of residual stresses, if σ_δ^{th} given by Eq. (6) (≈ 400 MPa) is compared with $\sigma_\delta^{residual}$ (≈ 300 MPa), only a fraction $R \approx 0.5$ of this energy can be really relaxed by the cracks. We assume that propagation occurs under constant critical conditions with mean energy release rate G_{lc} . An energy balance leads to^{19,20)}:

$$g L t_\delta G_{lc} = R S_0 E_\delta (\Delta\alpha)^2 (\Delta T)^2 t_\delta \quad (9)$$

where g is a geometrical correction factor which is likely to take into account the plane stress and plane strain contributions to crack propagation. Eq. (9) can be used to calculate a value of the crack network size d_c :

$$d_c = \frac{2gG_{lc}}{RE_\delta(\Delta\alpha)^2(\Delta T)^2} \quad (10)$$

Here, the calculated d_c value corresponds to a maximum, because the cracks of network I are propagated across the whole thickness of the δ layer. If the propagation could be limited up to a shorter depth $a < t_\delta$, the network would be denser and $d < d_c$. The Young's modulus of δ has been estimated from a mixture rule between those of Fe and Zn, according to the established applicability of this method for thermal expansion coefficients. By assuming that the g factor was not too different from 1, and using the $K_{lc}=2\text{MPa}\sqrt{\text{m}}$ value, as determined above, we obtained a d_c value of about $10\mu\text{m}$, which agreed rather well with the experimental observations. In addition, the experimentally observed d was found not to depend on the thickness of the δ layer, except when δ was very thin ($\leq 5\mu\text{m}$). In that condition, cracks were not clearly seen. It also agreed with Eq. (10).

3.3.2. Formation of crack network II

Under an external tensile stress σ_A , the mode I crack propagation is replaced by a mode II in δ of new cracks that originated from the former network I. As expected, the mode I crack propagation was stopped when arriving at the steel because of the large value of G_{lc}^α in α iron. The mean mode II propagation distance parallel to the α/δ interface was Δ . Sometimes several (β) II type cracks branch from the same I crack: the mean branching rate is denoted by β . In almost all cases, the mode II propagation occurred inside the δ phases and not at the α/δ interface as expected from the results obtained in other materials. Clearly, the reason for this lies in the atomic bonding between α and δ and its consequences on the plastic zone at the interface, which also depend on the plastic deformation of the most ductile phase. The following relationship between the energy release rates for mode II propagation in δ , α/δ and α may be written:

$$G_{lc}^\alpha < G_{lc}^{\alpha/\delta} < G_{lc}^\delta \quad (11)$$

If the atomic bonding between α and δ is broken by other phases (oxides, Γ ...), the critical energy release rate $G_{lc}^{\alpha/\delta}$ must be replaced by a value well smaller than G_{lc}^δ , therefore leading to delamination along the α/δ interface. For galvanizing, this is usually observed in the case of poor chemical surface pretreatment. If a fraction RII of the maximum energy W_{\max}^a is given by:

$$W_{\max}^\alpha = \frac{tg\sigma A^2 S_0}{2E_\delta} \quad (12)$$

is relaxed by the cracks propagating in δ and the following energy balance may be written:

$$L\beta G_{lc}\Delta = \frac{tg\sigma A^2}{2E_\delta} \quad (13)$$

As observed, the mode II propagation under external tensile stress σ_A can lead to the delamination of the coating. According to Eq. (13), the corresponding damage, D , defined for the fracture surface parallel to the interface ($LS0^{-1}\Delta$) is given by:

$$D = \frac{tg\sigma A^2}{2\beta E_\delta G_{lc}} \quad (14)$$

Although the former relationship has not been precisely verified, the experimental observations have clearly shown that D is a growing function of the thickness of the δ layer, t_δ , and of the externally applied energy, $\sigma_A^2/2E_\delta$.

The significance of the branching parameter β has to be considered in the context of continuum damage mechanics. It shows that in this case, as well as the toughening of the brittle systems, multiple cracking is less damaging than single crack propagation because in the former, the energy consumption is much larger than that in the latter.

Because the G_c , as well as the K_{lc} criteria, correspond, in fact, to the propagation of the cracks already formed in the material, there is the question of how cracks in δ are initiated. The most probable initiation process for cracks seems to be related to the morphology of mode I.

If only a stress criterion is considered for the crack formation and propagation, another equivalent description of the observed phenomena may be proposed. In an elastic determination of stresses σ_{el} developed during cooling, we showed that three zones could be considered (Fig. 7).

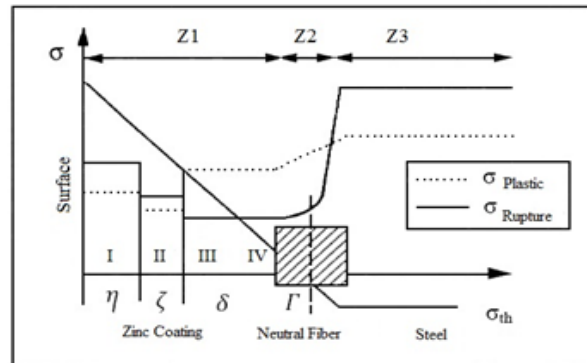


Fig. 8. Qualitative variation of σ_{th} thermal stress arising from cooling.

Z_1 corresponds to the major part of the coating; tensile stress varies nearly linearly with the depth. Z_2 corresponds to the vicinity of the steel-coating interface; calculation of stresses is imprecise and it is shown that the neutral fiber corresponding to $\sigma_{el}=0$ is near the Γ phase. Z_3 corresponds to the steel substrate; the stress field corresponds to weak compression. In the case of a hypo-sandelin coating for which the η , ζ and δ are clearly distinguished, Z_1 corresponds to three domains

inside which the plastic flow stresses σ_p^η , σ_p^ζ and σ_R^δ could be distinguished. By plotting qualitatively these stresses (Fig. 7), it is possible to show why cracks are formed at the upper part of δ , stopped in ζ and η and not propagated towards the substrate.

It is clear that delamination of the coating is delayed or prevented by the ductility of η zinc on the external part and the ductility of steel at the interface with the substrate. Therefore, when this ductility is suppressed, this conclusion has to be reconsidered, especially if the experimental conditions favor the propagation of the plastic zone in the ductile phases or the embrittlement of the substrate, which is likely to promote inter- or intra- granular cracking.

4. Conclusion

Experimental determination of the mechanical properties of each of different intermetallic compounds constituting the galvanizing coating led to model the behavior of the whole assembly. The results demonstrated that the phases present in the coating had different hardness values and that δ phase had a much higher hardness and smaller toughness value. Also, due to the differences in the thermal expansion coefficients of the coating and the substrate, complex residual thermal stresses were developed in the coating. The high value of hardness and residual thermal strain in δ phase led to the formation of cracks in the coating, as confirmed by both experimental observations and modeling. In the modeling, it was observed that in δ phase, the cracks grew in two modes, I, perpendicular to the δ/α interface, and II, parallel to the δ/α interface. Due to the flexibility of other layers of the coating as well as the steel substrate, development of cracks in δ phase was stopped and delamination of the coating was delayed.

References

- [1] J. Lu, X. Wang, C. Che, G. Kong, J. Chen, Q. Xu: *T. Nonferr. Metal. Soc.*, 17(2007), 351.
- [2] A. Azimi, F. Ashrafzadeh, M.R. Toroghinejad, F. Shahriari: *Eng. Fail. Anal.*, 26 (2012), 81.
- [3] I. Infante Danzo, K. Verbeken, Y. Houbaert: *Thin Solid Films*, 520 (2011), 1638.
- [4] H. Liu, F. Li, W. Shi, R. Liu, L Li: *Surf. Coat. Tech.*, 205 (2011), 3535.
- [5] A. R. Marder: *Prog. Mater. Sci.*, 45 (2000), 191.
- [6] J. Nakano, D. V. Malakhov, S. Yamaguchi, G. R. Purdy: *Computer Coupling of Phase Diagrams and Thermochemistry* 31 (2007), 125.
- [7] P. Rajak, U. Tewary, S. Das, B. Bhattacharya, N. Chakraborti: *Comp. Mater. Sci.*, 50 (2011), 2502.
- [8] E. M. Bellhouse and J. R. McDermid: *Mat. Sci. Tec and En. A*, 491(2008), 39.
- [9] T. H. Cook: *Met. Fin.*, 101(2003), 22.
- [10] T. J. Langill, B. Dugan: *Galvanized Steel Reinforcement in Concrete*, (2004), 87.
- [11] A. G. Evan: *J. Am. Ceram. Soc.*, 73(1990), 187.
- [12] K. M. Liang, G. Orange, G. Fantozzi: *J. Mat. Sci.*, 25(1990), 207.
- [13] C. B. Ponton, R. D. Rawlings: *Mat. Sci. Technol.*, 5(1989), 865.
- [13] B. R. Lawn, M. V. Swain: *J. Mat. Sci.*, 10(1975), 113.
- [14] A. G. Evans, E. A. Charles: *J. Am. Ceram. Sci.*, 59(1976), 371.
- [15] D. B. Marshall, B. R. Lawn: *J. Am. Ceram. Soc.*, 60(1977), 86.
- [16] J. T. Lu, X. Wang, C. S. Che, G. Kong, J. H. Chen, Q. Y. Xu: *T. Nonferr. Metal. Soc.*, 17(2007), 351.
- [17] S. Peng, J. Lu, C. Che, G. Kong, Q. Xu: *Ap. Sur. Sci.*, 256(2010), 5015.
- [18] *The strength of materials, part 1; Elementary theory and problems*, S. Timoshenko, Van Nostrand, Toronto, 1955.
- [19] J. Foct: *Scripta Met. et Mat*, 28(1993), 127.
- [20] S. M. Shibli, R. Manu: *Ap. Sur. Sci.*, 252(2006), 3058.